We are IntechOpen, the world's leading publisher of Open Access books Built by scientists, for scientists

4,800
Open access books available

122,000
International authors and editors

135M
Downloads

Our authors are among the

154
Countries delivered to

TOP 1%
most cited scientists

12.2%
Contributors from top 500 universities

CLARIVATE ANALYTICS BOOK CITATION INDEX INDEXED

WEB OF SCIENCE™

Selection of our books indexed in the Book Citation Index in Web of Science™ Core Collection (BKCI)

Interested in publishing with us?
Contact book.department@intechopen.com

Numbers displayed above are based on latest data collected.
For more information visit www.intechopen.com

21

Worm-like Locomotion Systems (WLLS) – Theory, Control and Prototypes

Klaus Zimmermann[1], Igor Zeidis[1], Joachim Steigenberger[1], Carsten Behn[1], Valter Böhm[1], Jana Popp[1], Emil Kolev[1] and Vera A. Naletova[2]
[1]*Technische Universität Ilmenau,* [2]*Moscow State University*
[1]*Germany*/[2]*Russia*

1. Introduction

Most of biologically inspired locomotion systems are dominated by walking machines - *pedal locomotion*. A lot of biological models (bipedal up to octopedal) are studied in the literature and their constructions were transferred by engineers in different forms of realization. *Non-pedal* forms of locomotion show their advantages in inspection techniques or in applications to medical technology for diagnostic systems and minimally invasive surgery (endoscopy). These areas of application were considered by (Choi et al., 2002), (Mangan et al., 2002), (Menciassi & Dario, 2003). Hence, this type of locomotion and its drive mechanisms are current topics of main focus.
In this chapter we discuss the problem of developing worm-like locomotion systems, which have the earthworm as a living prototype, from two points of view:

- modelling and controlling in various levels of abstraction,
- designing of prototypes with classical and non-classical forms of drive.

2. Motion and Control of WLLS

2.1 General Approach to WLLS

The following is taken as the basis of our theory:

i. A worm is a terrestrical locomotion system of one dominant linear dimension with no active legs nor wheels.
ii. Global displacement is achieved by (periodic) change of shape (such as local strain) and interaction with the environment.
iii. The model body of a worm is a 1-dimensional continuum that serves as the support of various fields.

The continuum in (iii) is just an interval of a body-fixed coordinate. Most important fields are: mass, continuously distributed (with a density function) or in discrete distribution (chain of point masses), actuators, i.e., devices which produce internal displacements or forces thus mimicking muscles, surface structure causing the interaction with the environment.

Source: Climbing & Walking Robots, Towards New Applications, Book edited by Houxiang Zhang,
ISBN 978-3-902613-16-5, pp.546, October 2007, Itech Education and Publishing, Vienna, Austria

Observing the locomotion of worms one recognizes first a surface contact with the ground. It is well known, that, if there is contact between two bodies (worm and ground), there is some kind of friction, which depends on the physical properties of the surfaces of the bodies. In particular, the friction may be anisotropic (depends on the orientation of the relative displacement). This interaction (mentioned in (ii)) could emerge from a surface texture as asymmetric Coulomb friction or from a surface endowed with scales or bristles (we shall speak of spikes for short) preventing backward displacements. It is responsible for the conversion of (mostly periodic) internal and internally driven motions into a change of external position (undulatory locomotion (Ostrowski et al., 2006)), see (Steigenberger, 1999) and (Zimmermann et al., 2003).
One of the first works in the context of worms, snakes and scales is the paper of (Miller, 1988). The author considers, in a computer graphics context, mass-spring systems with scales aiming at modelling virtual worms and snakes and their animations.
Summarizing, we consider a WLLS in form of a chain of point masses in a common straight line (**a discrete straight worm**), which are connected consecutively by linear visco-elastic elements, see (Behn, 2005), (Behn & Zimmermann, 2006) , (Zimmermann et al., 2002), (Zimmermann et al., 2003) for instance and Fig. 1.

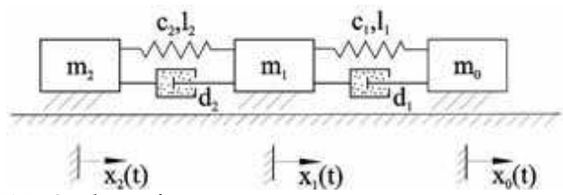

Fig. 1. Model of a WLLS - chain of point masses

In the next Subsection 2.2 we consider the case, where the point masses are endowed with scales, which make the friction orientation dependent (in sliding forward the frictional forces are minimal while in opposite direction the spikes dig in and cause large friction), see (Steigenberger, 1999) and (Steigenberger, 2004). In Subsection 2.3, due to (Behn, 2005) and (Behn & Zimmermann, 2006), we do not want to deal with reactive forces as before, instead we model this ground interaction as impressed forces - asymmetric (anisotropic) dry friction as a Coulomb sliding friction force, see (Blekhman, 2000).

2.2 Kinematic Theory of WLLS

In this subsection we focus on interaction via *spikes*.
The *kinematics* of this $DOF = n+1$ system formulates as follows.
The spikes entail the differential constraint

$$\dot{x}_i(t) \geq 0,\ i = 0,\ldots,n,\ \forall t \tag{1}$$

whence with $S_i = x_0 - x_i$ there holds $\dot{x}_0 \geq \dot{S}_i$ for all i and thus

$$\dot{x}_0 = V_0 + w,\ V_0 := \max\left\{\dot{S}_i,\ i = 0,\ldots,n\right\},\ w \geq 0. \tag{2}$$

w is a common part of the velocities, it describes a rigid motion of the system. The value w remains undetermined in kinematics, it only follows from dynamics.
The *dynamics* of the WLLS are governed by the momentum laws of the point masses,

$$m\ddot{x}_i = g_i + \mu_i - \mu_{i+1} + \lambda_i,\ i = 0,\ldots,n, \tag{3}$$

where the g_i are external physically given forces, μ_i are internal forces ($\mu_0 = \mu_{n+1} := 0$), whereas λ_i are the *reaction forces* corresponding to the *one-sided* constraint (1), so there hold the *complementary slackness conditions*

$$\dot{x}_i \geq 0,\ \lambda_i \geq 0,\ \dot{x}_i \cdot \lambda_i = 0. \tag{4}$$

Let $g_i + \mu_i - \mu_{i+1} =: f_i$, then for any motion (4) will be satisfied by the 'controller'

$$\lambda_i = -\frac{1}{2}(1 - sign(\dot{x}_i))(1 - sign(f_i))f_i. \tag{5}$$

Now let us suppose a *kinematic drive*, i.e., the actuators are assumed to precisely prescribe the mutual distances l_j as functions of time, see Fig. 2.

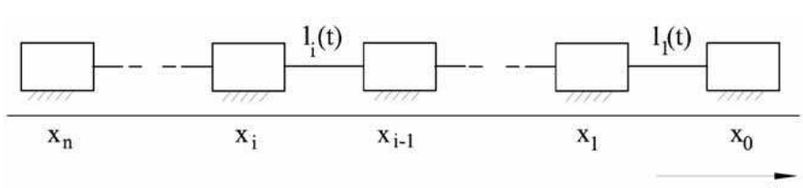

Fig. 2. WLLS with kinematic drive

The kinematic drive implies the *holonomic constraint*

$$x_{j-1} - x_j - l_j(t) = 0,\ j = 1,\ldots,n \tag{6}$$

with μ_j as respective reactions. $\dot{S}_i$ and V_0 are now given functions of time, the DOF of the system shrinks to *1*.
We confine the external forces to $g_i = -k\dot{x}_i - \Gamma$ then, summing up all the momentum laws (3) while observing $\dot{x}_i = V_0 - \dot{S}_i + w$ there follows a *bimodal ADE* for w and $\lambda := \frac{1}{n+1}\sum_0^n \lambda_i$,

$$\begin{aligned} &m\,\dot{w} + k\,w + \sigma(t) = \lambda, \qquad w \geq 0,\ \lambda \geq 0,\ w\lambda = 0, \\ &\sigma := m\dot{W}_0 + kW_0 + \Gamma, \quad W_0 := V_0 - \frac{1}{n+1}\sum_0^n \dot{S}_i. \end{aligned} \tag{7}$$

In mode 1 $\{w>0;\lambda=0\}$ no point mass is at rest whereas in mode 2 $\{w=0,\ \lambda>0\}$ at least one does not move (active spike). If we set $w=0$ then all what follows is called *kinematic theory*.

It is easy to deduce: *If* $\sigma(t)>0$ *for all t then the motion is always in mode 2, at any time at least one spike is active, the motion is well-determined by kinematics*.

We consider an example with $n=2$. The actuators are chosen so as to generate l_1 and l_2 as T-periodic piecewise cosine functions. This given gait will be reconsidered in Subsection 2.3. Fig. 3 shows l_1, l_2 vs. t/T (left), and with some system data m,k,Γ chosen the corresponding worm motion (right, t -axis upward).

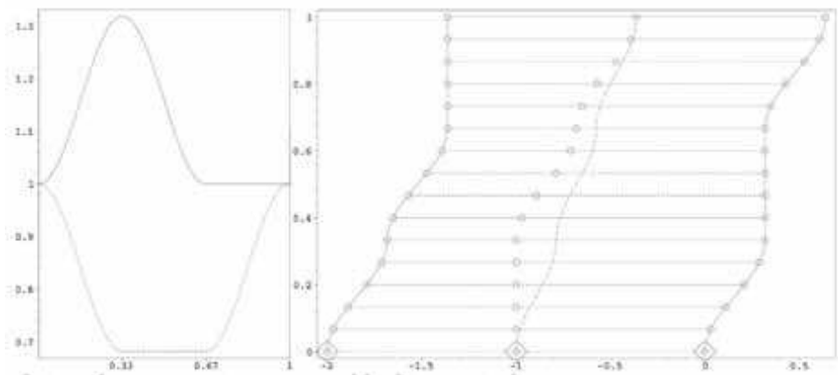

Fig. 3. Gait and worm motion governed by kinematic theory

Mind that one spike is active (resting point mass) at any time. So this gait might be suitable for motion 'in the plane'. An uphill gait (two resting point masses an any time) could easily be constructed, too (Steigenberger, 2004). To ensure $w=0$ and sufficiently small λ (to prevent the spikes from breakdown) certain restrictions for T and Γ must be obeyed, see (Steigenberger, 2004).

Two items deserve particular observation.

i. Using common actuators the proper control variable u is not l_i or $\dot{l}_i$ but rather an electrical voltage or a pressure applied to some piezo or hydraulic device that in turn acts to the point masses via some visco-elastic coupling. In this case there remains $DOF=n+1$ and the internal forces μ_j follow a law of the form

$$\mu_j = c\left(x_{j+1}-x_j\right)+d\left(\dot{x}_{j+1}-\dot{x}_j\right)+u_j(t). \tag{8}$$

ii. By chance it could practically be promising to consider asymmetric dry friction instead of spikes (though the simple kinematical theory then is passé). In a rough terrain, unknown or changing friction coefficients lead to uncertain systems and require adaptive control to track a kinematic gait, that has been decovered as a favourable one. This objective will be addressed in the next section.

2.3 WLLS as a Dynamical Control System

In this subsection we model the ground interaction as an **asymmetric Coulomb dry friction force** F (see above), which is taken to be different in the magnitude depending on the direction of each point mass motion:

$$\dot{x} \mapsto F(\dot{x}) = \begin{cases} -F^{+} & , \dot{x} > 0 \\ F^{0} & , \dot{x} = 0 \\ F^{-} & , \dot{x} < 0 \end{cases} \tag{9}$$

where $F^{+}, F^{-} > 0$ are fixed with $F^{-} >> F^{+}$ and F^{0} is arbitrary , $F^{0} \in \left(F^{-}, -F^{+}\right)$.

For later simulation we restrict the number of point masses to $n = 2$, but we point out that our theory is valid for fixed but arbitrary $n \in N$, see (Behn & Zimmermann, 2006).

Mathematical model

Firstly, we derive the differential equations of motion of the WLLS by using Newton's second law:

$$\begin{aligned} m_0\ddot{x}_0 &= -c_1(x_0 - x_1) - d_1(\dot{x}_0 - \dot{x}_1) + F_0(\dot{x}_0) + u_1(t) \\ m_1\ddot{x}_1 &= \begin{cases} -c_1(x_1 - x_2) + c_2(x_0 - x_1) - d_1(\dot{x}_1 - \dot{x}_2) + d_2(\dot{x}_0 - \dot{x}_1) \\ \quad + F_1(\dot{x}_1) + u_2(t) - u_1(t) \end{cases} \\ m_2\ddot{x}_2 &= c_2(x_1 - x_2) + d_2(\dot{x}_1 - \dot{x}_2) + F_2(\dot{x}_2) - u_2(t) \end{aligned} \tag{10}$$

with $x_0(0) = x_{00}$, $x_1(0) = x_{10}$, $x_2(0) = x_{20}$, $\dot{x}_0(0) = x_{01}$, $\dot{x}_1(0) = x_{11}$, $\dot{x}_2(0) = x_{21}$ (all initial values are real numbers) and $g_i = 0$. Putting

$$u_1 := c_1 l_1 \text{ and } u_2 := c_2 l_2 \tag{11}$$

then u_{ij} is in fact a control of the original spring length. Therefore, we have *internal* inputs and no longer external force inputs, as in (Behn, 2005). New outputs of this system could be the actual distances of the point masses

$$y_1 := x_0 - x_1 \text{ and } y_2 := x_1 - x_2 . \tag{12}$$

Therefore, this system (10), (12) is described by a mathematical model that falls into the category of quadratic, nonlinearly perturbed, minimum phase, multi-input $u(\cdot)$, multi-output $y(\cdot)$ systems with strict relative degree two. In a normalized form (after elaborate transformations) the zero dynamics of the system are decoupled from the controlled part of the system.

Control Objective

For the further analysis of this system we suppose that the masses are all equal, but unknown, also the damping factors and spring stiffnesses, and the friction magnitudes as well (**uncertain systems**).
The consideration of uncertain systems leads to the use of adaptive control. The aim is to design universal adaptive controllers, which learn from the behavior of the system, so automatically adjust their parameters and achieve a pre-specified control objective. Simple adaptive mechanisms, which achieve tracking of a given reference signal within any pre-specified accuracy λ, will be introduced. $\lambda > 0$ denotes the size of the feasible tracking error (we do not focus on exact tracking).
Precisely, given an arbitrarily small $\lambda > 0$, a control strategy $y \mapsto u$ is sought which, when applied to the system, achieves λ-tracking (λ-*tracking control objective*) for every reference signal $y_{ref}(\cdot)$ (belonging to a certain function class, for instance a given favoured kinematic gait presented in the previous subsection), i.e., the following:

i. every solution of the closed-loop system is defined and bounded on $R_{\geq 0}$, and
ii. the output $y(\cdot)$ tracks $y_{ref}(\cdot)$ with asymptotic accuracy quantified by $\lambda > 0$ in the sense that $\max\left\{0, \left\| y(t) - y_{ref}(t) \right\| - \lambda \right\} \to 0$ as $t \to +\infty$.

The last condition means that the error $e(t) := y(t) - y_{ref}(t)$ is forced, via the adaptive feedback mechanism (controllers (13) and (14)), towards a ball around zero radius $\lambda > 0$, see Fig. 4.

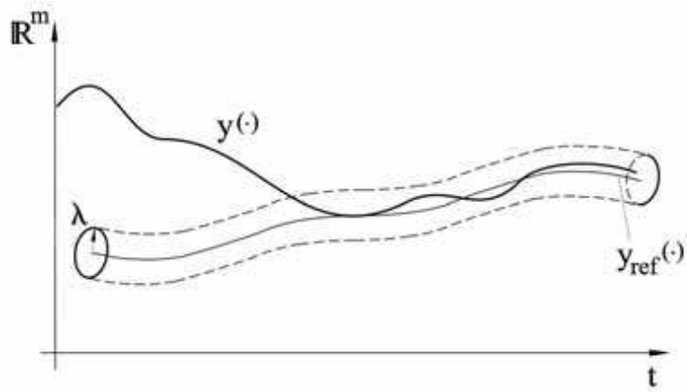

Fig. 4. The λ-radius around the reference signal

Controllers

Let us consider the following two λ-trackers, see also (Behn, 2005).

$$\left.\begin{array}{rcl} e(t) & := & y(t)-y_{ref}(t) \\ u(t) & = & -\left(k(t)\,e(t)+\frac{d}{dt}[k(t)\,e(t)]\right) \\ \dot{k}(t) & = & \left(\max\{0,\|e(t)\|-\lambda\}\right)^2 \end{array}\right\} \tag{13}$$

with $k(0)=k_0\in R$, $\lambda>0$, $y_{ref}(\cdot)\in W^{2,\infty}$ (a Sobolev-Space), $u(t), e(t)\in R^2$ and $k(t)\in R$.

The second one includes a dynamic compensator due to a controller of (Miller & Davison, 1991). This controller allows us to avoid the drawback of using the derivative of the output, mentioned above, in the following way:

$$\left.\begin{array}{rcl} e(t) & := & y(t)-y_{ref}(t) \\ u(t) & = & -\left(k(t)\,\vartheta(t)+\frac{d}{dt}[k(t)\,\vartheta(t)]\right) \\ \dot{\vartheta}(t) & = & -k(t)^2\,\vartheta(t)+k(t)^2\,e(t) \\ \dot{k}(t) & = & \left(\max\{0,\|e(t)\|-\lambda\}\right)^2 \end{array}\right\} \tag{14}$$

with $\theta(0)=\vartheta_0$, $k(0)=k_0>0$, $\lambda>0$, $y_{ref}(\cdot)\in W^{2,\infty}$, $u(t), e(t), \vartheta(t)\in R^2$ and $k(t)\in R$.

We stress, that the controller (14) does not invoke any derivatives.
The structure of the feedback law and the simple adaptation law of the controllers in this subsection already exist in the literature, but they were only applied to systems with relative degree one. The considered WLLS has relative degree two. Therefore, the novelty is the application of the controller to systems with relative degree two. There are only a few papers which focus the adaptive λ-tracking problem for system with relative degree two, but the feedback law here is simpler than the introduced ones in (Dragan & Halanay, 1999), (Ye, 1999), (Miller & Davison, 1991).
These controllers achieve λ-tracking (for the proofs the reader's attention is invited to (Behn, 2005)) as presented in the following simulations. We apply both controllers (13) and (14) to system (10), (12) to track the given gaits.

2.4 Simulations

In this subsection we apply the presented simple adaptive λ-tracking control strategies to our WLLS (dynamical control system) in order to track given reference signals. Firstly, we try to track a time-shift $\sin(\cdot)$-signal, and, second, a kinematic gait developed in (Steigenberger, 2004) to achieve a certain movement of the WLLS. The numerical simulations will demonstrate and illustrate that the adaptive controllers work successfully and effectively. We point out, that the adaptive nature of the controllers is expressed by the arbitrary choice of the system parameters. It is obvious that for numerical simulation the system data have to be chosen fixed and known, but the controllers are able to adjust their gain parameter to each set of system data.
The tracking results when applying controller (13) to our WLLS are already presented in (Behn & Zimmermann, 2006). Therefore, we choose the same parameters (dimensionless) as there to obtain comparable simulations in using the second controller (14). Then we have:

- system: $m_0 = m_1 = m_2 = 1$, $c_1 = c_2 = 10$, $d_1 = d_2 = 5$, $x_{00} = 0$, $x_{10} = 2$, $x_{20} = 4$, $x_{01} = 0$, $x_{11} = 0$, $x_{21} = 0$;
- Coulomb friction forces: $F^+ = 1$, $F^- = 10$, hence we have by an approximation $v_i \mapsto 5.5\tanh(40 v_i) - 4.5$, $i = 0,\ldots,2$;
- λ-tracker (controller): $\lambda = 0.2$, $k_0 = 1$, $\vartheta_1(0) = 1$, $\vartheta_2(0) = 1$.

In order to detect differences we present the simulation results with the λ-trackers (14) and (13), respectively, side by side.

Tracking of a Gait Presented in Fig. 3, left

This gait is derived from the theory of a chain of point masses with spikes and links of given t-dependent lengths. Such a theory is essentially kinematical and does not require dynamics from the very beginning, see Subsection 2.2. In (Steigenberger, 2004) two paradigmatic gaits for a three point system were derived such that at any time during motion the same (prescribed) number of spikes is active: one in a fast `in-plane gait', two in a slow `up-hill gait'. We try to track this fast gait in our dynamical theory, it is for $t \in [0,1]$:

$$t \mapsto y_{ref}(t) = \begin{pmatrix} \begin{cases} l_0[1-\varepsilon(-1+\cos(3\pi t))] & , t \in [0,2/3) \\ l_0 & , t \in [2/3,1) \end{cases} \\ \begin{cases} l_0[1-\varepsilon(1-\cos(3\pi t))] & , t \in [0,1/3) \\ l_0[1-2\varepsilon] & , t \in [1/3,2/3) \\ l_0[1-\varepsilon(1+\cos(3\pi t))] & , t \in [2/3,1) \end{cases} \end{pmatrix}, \tag{15}$$

where l_0 is the original length (dimensionless chosen as 2 units) and $2\varepsilon = 0.3$ is the elongation. This gait is periodically repeated. We obtain the following simulations.

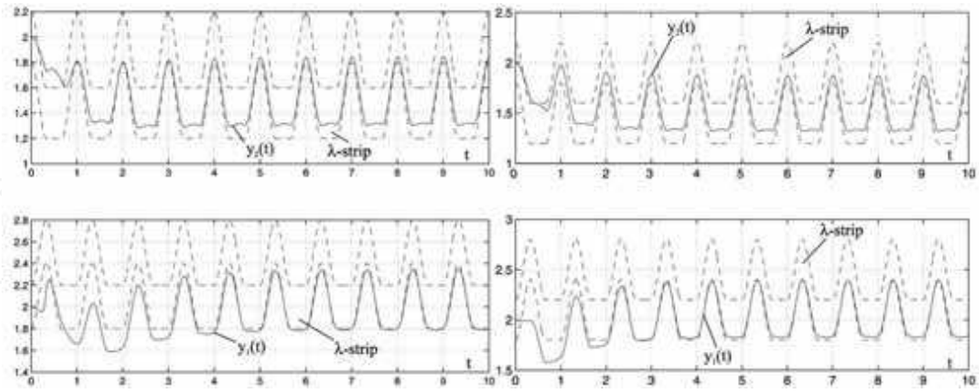

Fig. 5. Outputs and λ-strips – left: for (14), right: for (13)

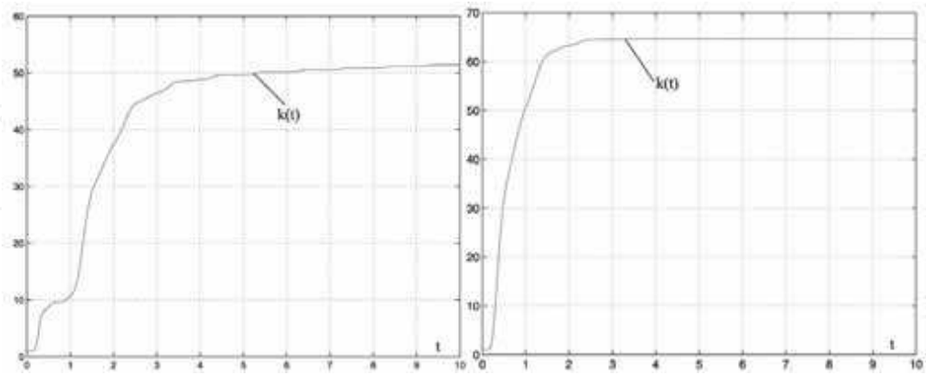

Fig. 6. The gain parameters - left: for (14), right: for (13)

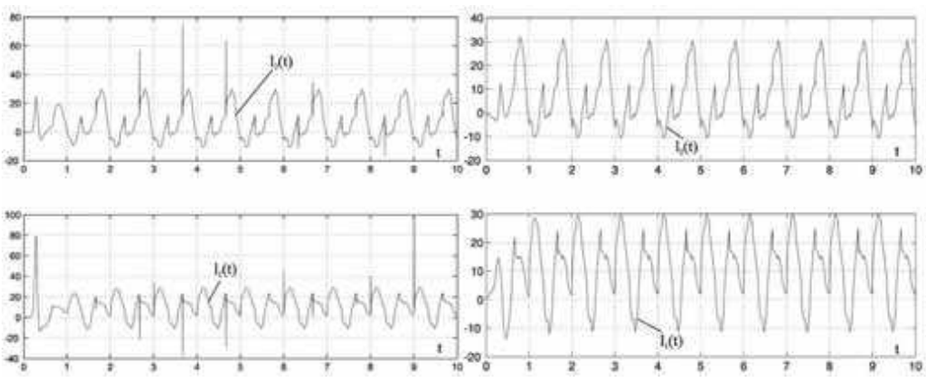

Fig. 7. The control inputs - left: for (14), right: for (13)

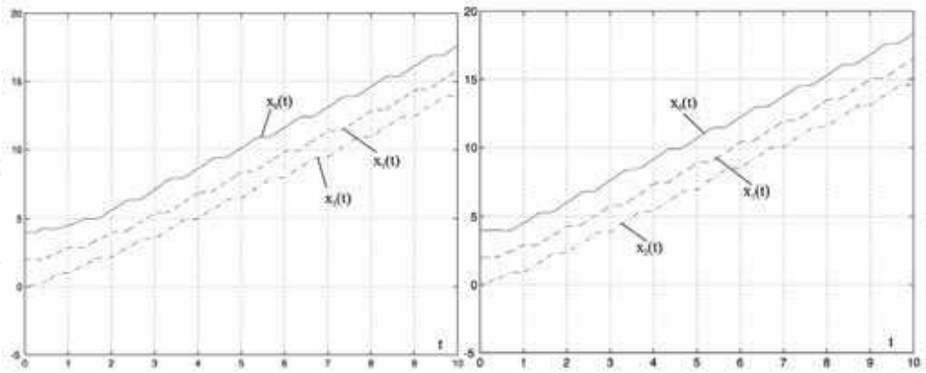

Fig. 8. The motions of the worm - left: with (14), right: with (13)

Fig. 5 shows the outputs of the systems and the according λ-strips. The reference signal is tracked very quickly with controller (13) in comparison to controller (14). In Fig. 5, left, the

outputs are not captured yet. The gain parameters, shown in Fig. 6, increase as long as the outputs are outside the λ-strips. Fig. 7 shows the necessary control inputs, and Fig. 8 the corresponding motions of the worm.
It can be seen that controller (13) works more effectively than controller (14) because we feed back more information about the output derivative than (14), which has to estimate the derivative. Hence, in the simulation with controller (14) , the outputs are not captured on the considered time interval and the gain parameter is still increasing. Fig. 6, right, clearly shows the convergence of the gain parameter in the simulation with controller (13).

2.5 Electromechanical Prototype

A prototype was designed in order to check the above-mentioned theory (Abaza, 2006). It consists of two stepping motors and a dummy to produce a three point mass worm system (Fig. 9). Each stepping motor can separately travel along a threaded rod in both directions with different controllable speeds to generate $\dot{l}_i$.

Fig. 9. Three point mass worm system

Additionally, a special bristle-structure had been integrated (Fig. 10) to prevent the point masses from slipping backwards. Experiments justified the results of the theory.

Fig. 10. The bristle-structure

2.6 Open Problems

The following problems should be considered for future work:

- algorithms to construct preferable kinematic gaits;

- to include a suitable friction law allowing for stiction;
- revised control objectives
  - keep spikes (improved Coulomb friction with a big stiction coefficient for negative velocities F_0^-);
  - prescribe $y_{ref}(\cdot)$ as a kinematic gait;
  - let c_i and d_i be random (possibly t-dependent).

3. WLLS Using Deformable Magnetizable Media

3.1 Introductional Remarks

The realization of locomotion systems using the deformation of magnetizable materials (a magnetic fluid or a magnetizable polymer) in a magnetic field is an actual problem. The initiator of motion in such devices is an alternate magnetic field, which forms to exterior sources (electromagnetic system or motion permanent magnets). In (Zimmermann et al., 2004a, b) the theory of a flow of layers of magnetizable fluids in a travelling magnetic field is considered. It is shown, that the travelling magnetic field can create a flux in the fluid layers. This effect can be applied for the realization of locomotion. A micro-robot with individual cells corresponding to the earthworm's segment and sealed with water-based magnetic fluid is developed by (Saga & Nakamura, 2002, 2004).

In the present chapter theoretical and experimental possibilities of using deformable magnetizable media as actuators for mobile robots are investigated.

In the subsection 2.5 a classical electromechanical drive was used for controlling the distance between the two masses of the WLLS. In (Zimmermann et al. 2003) we considered a system of two masses connected by a piezo element. In the following second subsection we used a magneto-elastic element as an internal drive. The undulatory locomotion of an biological inspired artificial worm is based on travelling waves on its surface. Therefore the expression for the magnetic field strength creating a sinusoidal wave on the surface of a viscous magnetic fluid as a function of the characteristics of the fluid (viscosity, surface tension, and magnetic permeability) and the parameters of the wave are obtained in the third also theoretically oriented subsection of this section. In the fourth subsection the motions of three samples of a magnetizable body (magnetizable worm) in an alternate magnetic field are studied experimentally for large diapason of the electromagnetic system frequency. The prolate bodies of the magnetizable composites (an elastic polymer and solid magnetizable particles) and a capsule with a magnetic fluid are used. The analytical estimation and numerical calculation of the deformation of the bodies in applied magnetic field and of the velocity of the bodies are done. A deformable magnetizable worm in a magnetic field is a prototype of a mobile crawling robot. Such devices have some characteristics, which allow to use them in medicine and biology. For example, it does not contain solid details contacting with a surrounding medium and it moves autonomously.

The fives subsection deals with fundamental investigations necessary for the design and the application of segmented artificial worms, which have the earthworm as living prototype, and of new passive locomotion systems. A important question in this interconnection is the estimation of the pressure distribution in the magnetic fluid under the influence of a controlled magnetic field.

3.2 Modelling of WLLS with Magneto-Elastic Elements

In (Turkov, 2002) a deformation of the elastic composite body, when a magnetic field is applied, is considered. A formula, which allows to calculate the deformation of a parallelepiped in noninductive approximation was obtained. f the Lame coefficients λ and η satisfy the condition $\lambda >> \eta$ then relative lengthening in the direction of the axis OX (for small strains), when magnetic field $\mathbf{H} = \mathbf{H}_0$ in orthogonal direction is applied, is given by expression $u = \frac{p}{E_y^{eff}} + u_0$ (Fig. 11). Here p is the density of surface force, u_0 is the deformation of the sample, produced by the action of the magnetic field only in absence of force ($p = 0$), E_y^{eff} is the effective value of the Young modulus

$$u_0 = \frac{\mu_0 \left[2\left(\mu^0 - 1\right) - a_1\right] H^2}{12\eta\left(1 + \frac{2}{3}G\right)} > 0, \quad E_y^{eff} = 3\eta \frac{\left(1 + \frac{2}{3}G\right)}{\left(1 + \frac{1}{2}G\right)}, \quad G = \frac{\mu_0 a_1 H_0^2}{2\eta}.$$

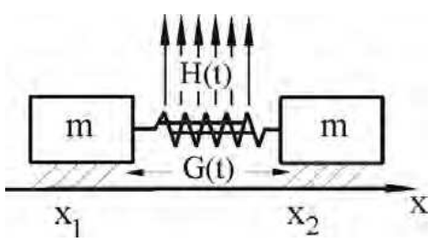

Fig. 11. Model of a WLLS with two mass points, non-symmetric Coulomb friction and a periodic internal force $G(t)$ produced by an external magnetic field H

The value $\mu_0 = 4\pi \times 10^{-7}\, N/A^2$ is the permeability of free space, μ^0 is the permeability of the unstrained material, $a_1 = -\frac{2}{5}\left(\mu^0 - 1\right)^2$. By the action of a magnetic field the sample of the composite with a drop of a magnetic fluid lengthens, and the value modulus E_y^{eff} in a magnetic field has to become less than without a magnetic field. The experimental dependencies between the stress and the strain without influence of field ($H = 0$) and with influence of a field ($H = 1{,}5 \cdot 10^5$ A/m) for a sample with the length $l_0 = 29\, mm$ and the area of cross section $S_0 = 5.5\, mm^2$ is shown in Fig. 12.

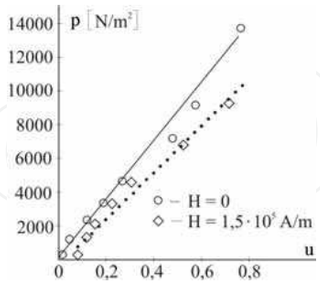

Fig. 12. Stress p vs. strain u

The size of the ferromagnetic particles in the magnetic fluid is about 110 Å. The experiment allowed us to define $u_0 = u(0) = 0{,}071$.

The motion of a system of two material points x_1 and x_2 with the masses m , connected by a spring of stiffness $c = E_y^{eff} \cdot S_0 / l_0$ ($\omega^2 = c/m$) along an axis x is considered (Fig. 11). It is supposed that the points are under the action of a small non-symmetric Coulomb dry frictional force $mF(\dot{x})$, depending on velocities $\dot{x} = \dot{x}_i (i = 1,2)$, where $F(\dot{x}) = F^+$ if $\dot{x} > 0$, $F(\dot{x}) = -F^-$ if $\dot{x} < 0$, $F(\dot{x}) = F_0$ if $\dot{x} = 0$; $-F^- < F_0 < F^+$, $F^- \geq F^+ \geq 0$. By influence of an external harmonic magnetic field a small harmonic internal forces is produced: $G(t) = \frac{1}{2} u_0 c l_0 (1 + \cos\psi), \psi = \nu t$. We introduce the dimensionless variables (the dimensional variables are denoted here with the asterisk): $x_1, x_2 = x_1^*, x_2^* / l_0$, $t = t^* \omega$, $\nu = \nu^* / \omega$, $F = F^* / \left(\frac{1}{2} u_0 l_0 \omega^2\right)$, $\varepsilon = \frac{1}{2} u_0 << 1$. The dimensionless equations of the motion are:

$$\begin{aligned} \ddot{x}_1 + x_1 - x_2 &= -\varepsilon [F(\dot{x}_1) + (1 + \cos\psi)], \\ \ddot{x}_2 + x_2 - x_1 &= -\varepsilon [F(\dot{x}_2) - (1 + \cos\psi)]. \end{aligned} \tag{16}$$

To the system (16) we apply the procedure of averaging. For this purpose we introduce new variables: the velocity of the center of mass $V = (\dot{x}_1 + \dot{x}_2)/2$ and the deviation relatively to the center of mass $z = (x_2 - x_1)/2$. Replacing $z = a\cos\varphi$, $\dot{z} = -a\Omega\sin\varphi$, $\varphi = \Omega t + \vartheta$, $\Omega = \sqrt{2}$ where V, a, ϑ - slow variables, we receive system (16) in a standard form:

$$\begin{aligned} \dot{V} &= -\frac{\varepsilon}{2} [F(V + a\Omega\sin\varphi) + F(V - a\Omega\sin\varphi)], \\ \dot{a} &= -\frac{\varepsilon}{2\Omega} \sin\varphi [F(V + a\Omega\sin\varphi) - F(V - a\Omega\sin\varphi) + 2(1 + \cos\psi)], \\ \dot{\varphi} &= \Omega - \frac{\varepsilon}{2a\Omega} \cos\varphi [F(V + a\Omega\sin\varphi) - F(V - a\Omega\sin\varphi) + 2(1 + \cos\psi)], \\ \dot{\psi} &= \nu . \end{aligned} \tag{17}$$

We investigate the system (17) in a vicinity of the main resonance $\nu = \Omega + \varepsilon\Delta$ ($\Delta \neq 0$), introducing a new slow variable $\xi = \psi - \varphi$. After averaging on a fast variable φ we obtain:

$$\dot{V} = \begin{cases} -\varepsilon\left(\dfrac{F^- + F^+}{\pi}\arcsin\dfrac{V}{a\Omega} - \dfrac{F^- - F^+}{2}\right) & if\ 0 \le V < a\Omega, \\ -\varepsilon F^+ \quad if\ V \ge a\Omega, \end{cases}$$

$$\dot{a} = \begin{cases} -\dfrac{\varepsilon}{\Omega}\left(\dfrac{F^- + F^+}{\pi}\sqrt{1 - \dfrac{V^2}{a^2\Omega^2}} + \dfrac{a}{2}\sin\xi\right) & if\ 0 \le V < a\Omega, \\ -\varepsilon\dfrac{a}{2\Omega}\sin\xi \quad if\ V \ge a\Omega, \end{cases} \tag{18}$$

$$\dot{\xi} = \varepsilon\left(-\frac{1}{2\Omega}\cos\xi + \Delta\right).$$

We are interested in an approximately steady motion as a single whole, therefore we seek for the solution $\dot{V} = 0$. Then from system (18) we have $\dot{a} = \dot{\xi} = 0$ and

$$V = \frac{\sin\Phi}{|\Delta|}\sqrt{\frac{1}{4} - E^2\cos^2\Phi}, \quad a = \frac{1}{\Omega|\Delta|}\sqrt{\frac{1}{4} - E^2\cos^2\Phi}, \quad E\cos\Phi \le \frac{1}{2},$$
$$\xi = \arccos\left[-\frac{2\Delta}{|\Delta|}\sqrt{\frac{1}{4} - E^2\cos^2\Phi}\right], \quad E = \frac{F^- + F^+}{\pi}, \quad \Phi = \frac{\pi}{2}\cdot\frac{F^- - F^+}{F^- + F^+}. \tag{19}$$

The result of the numerical integration of the exact system (1) is given in Figure 13.

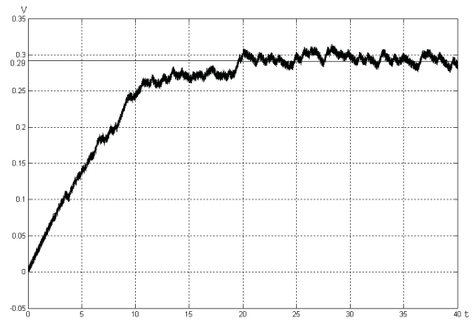

Fig. 13. Velocity V vs. time t

The following values of parameters for a magneto-elastic sample as described in Section 1 are taken: $m = 3\times10^{-3}kg$, $E_y^{eff} = 1.6\times10^4\ N/m^2$, $u_0 = 0.071$, $l_0 = 29\,mm$, $S_0 = 5.5mm^2$, $\omega = 32\,s^{-1}$. So, the values of the parameters are: $\varepsilon = 0.036$, $F_+ = 0.5$, $F_- = 1$, $\Delta = 0.5$. The

formula (4) gives the value for the dimension velocity of center of mass $V = 0.29 m/s$. The average velocity of such locomotion systems depends on the difference of the friction coefficients between the system and the substrate, which depends on the directions of motion.

3.3 Locomotion Using a Magnetic Fluid in a Traveling Magnetic Field

We consider a plane flow of an incompressible viscous magnetic fluid layer along a horizontal surface in a non uniform magnetic field (see Fig. 14). The magnetic permeability of the fluid μ is assumed to be constant. The pressure on the free fluid surface is constant. In the case of a constant magnetic permeability, the body magnetic force is absent and the magnetic field manifests itself in a surface force acting on the free surface (Rosensweig, 1985).

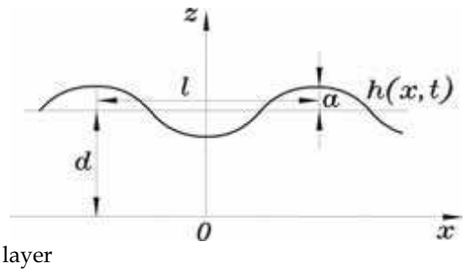

Fig. 14. Magnetic fluid layer

The gravity is not taken into account. In this case, the system of equations consists of the continuity and Navier-Stokes equations:

$$\operatorname{div} \mathbf{V} = 0, \quad \frac{\partial \mathbf{V}}{\partial t} + (\mathbf{V}\nabla)\mathbf{V} = -\frac{1}{\rho}\operatorname{grad} p + \frac{\eta}{\rho}\Delta \mathbf{V}. \tag{20}$$

Here, $\mathbf{V}$ is the velocity vector (u and w are the horizontal and vertical coordinates), p is the fluid pressure, η is the dynamic fluid viscosity coefficient, ρ is the fluid density, and t is time.

On the rigid substrate $z = 0$, the no-slip condition is satisfied:

$$\mathbf{V}(z = 0) = \mathbf{0} \tag{21}$$

On the free surface $z = h(x,t)$, conditions of two types, kinematic and dynamic ones, should be satisfied. The kinematic condition is of the form:

$$\frac{dh}{dt} = \frac{\partial h}{\partial t} + u\frac{\partial h}{\partial x} = w \tag{22}$$

The dynamic conditions of continuity of the normal and tangential stresses on the free surface $z = h(x,t)$ take the form (neglecting the influence of the environment)

$$\left[-p + \gamma\frac{1}{R} + \frac{B_n^2}{8\pi}\left(\frac{1}{\mu} - 1\right) - \frac{H_t^2}{8\pi}(\mu - 1)\right]\mathbf{n} + \tau_{ij} n^j \mathbf{e}^i = \mathbf{0}. \tag{23}$$

Here, τ_{ij} are the viscous stress tensor components, R is the radius of curvature of the surface $z=h(x,t)$, $\mathbf{n}$ is the vector of outward normal to the surface, $\mathbf{e}^j$ are the basis vectors, γ is the film surface tension coefficient, $B_n=\mu H_n$ is the normal component of the magnetic field strength vector. The magnetic field $\mathbf{H}$ is assumed to be fixed, since the non-inductive approximation implies $\mu-1<<1$.

We will assume that the magnetic field creates the periodic travelling wave on the surface of a sufficiently thin layer (we denote the dimensional variables with the asterisk *):

$$h^*(x,t)=d+a\cos\left(\omega t^*-kx^*\right),\quad \varepsilon=d\cdot k<<1. \tag{24}$$

We introduce the dimensionless variables

$$\begin{aligned} &x=x^*\cdot k,\ z=z^*/d,\quad h=h^*/d,\quad \delta=a/d,\quad u=u^*/U_c,\quad w=w^*U_c/\varepsilon,\quad U_c=\omega/k,\\ &t=t^*\cdot\omega,\quad p=p^*/P,\quad P=\eta\omega/\varepsilon^2,\quad H^2=H^{*2}/P,\quad Re=\rho U_c d/\eta,\quad W=\gamma d k^2/P. \end{aligned} \tag{25}$$

For $\varepsilon<<1$, we will seek for a solution in the form of a power series in ε ($A\equiv h,u,w,p$):

$$A(x,z,t)=A_0(x,z,t)+\varepsilon\cdot A_1(x,z,t)+\ldots. \tag{26}$$

In the zeroth approximation in ε, for $Re<1$ and $W=O(1)$, using the equations (20) and the condition (21) – (23), we obtain an expression for the velocity components (subscript "0" is omitted):

$$u(x,z,t)=F(x,t)\left(\frac{z^2}{2}-hz\right),\quad w(x,z,t)=F(x,t)\frac{\partial h}{\partial x}\cdot\frac{z^2}{2}+\frac{\partial F}{\partial x}\left(\frac{h}{2}\cdot\frac{z^2}{2}-\frac{z^3}{6}\right), \tag{27}$$

where $F(x,t)=\dfrac{\partial p}{\partial x}$.

The mass conservation law (20), condition (22), expression (24), and the assumption that $h(x,t)=h(\xi),\quad \xi=t-x$ imply the following equation for the flow rate Q:

$$\frac{\partial h}{\partial t}+\frac{\partial Q}{\partial x}=0,\quad Q(x,t)=-Fh^3/3=h+C. \tag{28}$$

If the flow is T-periodic, we can introduce the average flow rate: $\overline{Q}(x)=\dfrac{1}{T}\int_0^T Q(x,t)\,dt$. For $h(\xi)=1+\delta\cos(\xi)$, the dimensionless average flow rate is $\overline{Q}=1+C$.

Relation (23), with respect to (24), implies

$$W\frac{\partial^3 h}{\partial\xi^3}+\frac{(\mu-1)}{8\pi}\frac{\partial H^2}{\partial\xi}=-\frac{3}{h^2}-\frac{3C}{h^2}. \tag{29}$$

Using equation (29) it is possible to find the magnetic field creating the prescribed film shape:

$$H^2 = H_0^2 + \frac{8\pi}{\mu - 1}\left(-W\frac{\partial^2 h}{\partial \xi^2} - 3\int \frac{1}{h^2} d\xi - 3C\int \frac{1}{h^3} d\xi \right), \quad h(\xi) = 1 + \delta\cos(\xi), \quad \delta < 1. \tag{30}$$

The requirement for the magnetic field magnitude to change periodically leads to the expression $C = -2\left(1 - \delta^2\right)/\left(2 + \delta^2\right)$. The dependence of the average volume flow rate $\overline{Q} = 1 + C$ on the surface oscillation amplitude δ is shown in Fig. 15. The expression for the magnetic field (26) takes the form

$$H^2 = H_0^2 - D, \quad D = \frac{8\pi}{\mu - 1}\left(-W\delta\cos(\xi) + \frac{3\delta\sin(\xi)(2 + \delta\cos(\xi))}{(2 + \delta^2)(1 + \delta\cos(\xi))^2} \right). \tag{31}$$

The constant H_0^2 can be chosen arbitrarily. However, this constant must not be less than the maximum value, $D_{\max} > 0$, of the function D in order not to violate the condition $H^2 \geq 0$. Thus we can assume $H_0^2 = D_{\max}$.

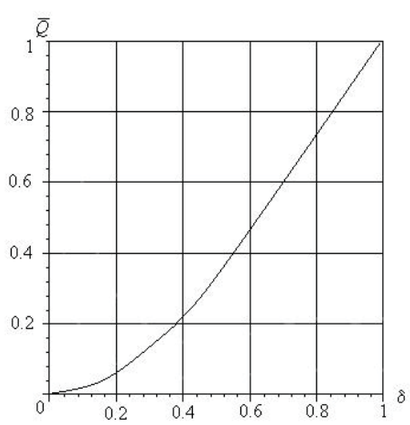

Fig. 15. Average volume flow rate $\overline{Q}$ vs. surface oscillation amplitude δ

3.4 Magnetizable Bodies in an Alternate Magnetic Field

In the experiments we use cylindrically-shaped bodies 01located in a cylindrical channel. The channel diameter d exceeds that d_w of the body. We denote the length of the body as l_w. The magnetic field is created by coils. The axes of the coils are in the horizontal plane, L is the distance between the axes of the coils and I is the current in the coils (see Fig. 16).
The coils are placed at the left and right hand sides of the channel. Magnetic field is created by three coils simultaneity (for example, coils numbers 6 - 8 in Fig. 16), the axis of the middle coil is the symmetry axis of the magnetic field.

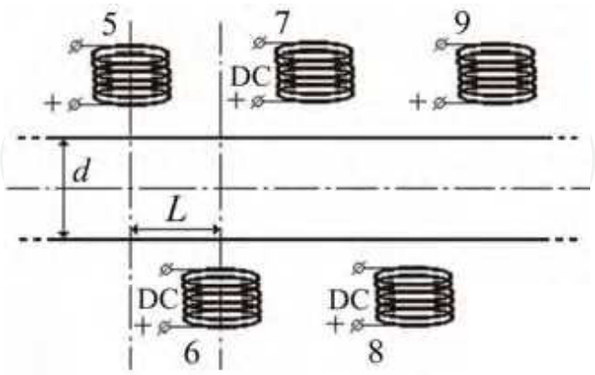

Fig. 16. Arrangement of coils of the electromagnetic system

Periodically, the left coil is switched off and the next coil is switched on, n is the number of the coil switches per second (the frequency), so $T = 1/n$ is the period between change-over of the coils. Currents flowing through the coils are unidirectional. Such an electromagnetic system forms a travelling magnetic field $\mathbf{H}$, which is a complex function of x, y, z, t (x is the coordinate along the channel, z is parallel to axis of the coils, y is orthogonal to x and z).
It is shown experimentally that in such periodic magnetic field the cylindrical magnetizable bodies move along the channel. The direction of the body motion is opposite to the direction of the travelling magnetic field.

The Bodies from a Magnetizable Polymer

In the first experiment $I = 4.6\text{A}$, $L = 10\text{mm}$, $d = 11\text{mm}$ and the parameters of the "worm" (sample 1) are as follows: Young's modulus $E_y = 50000\text{Pa}$, length $l_w = 48\text{mm}$, diameter $d_w = 4\text{mm}$. The frequency n changes from 5s^{-1} to 1000s^{-1} in this experiment. In the second experiment the parameters are $I = 4.6\text{A}$, $L = 10\text{mm}$, $d = 10\text{mm}$, $l_w = 75\text{mm}$, $d_w = 4.5\text{mm}$ and the sample 2 consists of a polymer with Young's modulus $E_y = 22000\text{Pa}$. The frequency n changes from 5s^{-1} to 1000s^{-1}. A cycle of body deformation by the travelling magnetic field is the process when the travelling magnetic field covers the body (see Fig. 17). At the end and beginning of this process the body is not deformed.

Fig. 17. Magnetizable elastic body (sample 1) in the travelling magnetic field

Elastic Capsule Filled with a Magnetic Fluid

In a third experiment an elastic cylindrical capsule filled with a magnetic fluid is in-side a cylindrical channel. The channel and capsule diameters (d, d_c) are 10mm and 4mm. The length of the capsule filled with a magnetic fluid l_c is 75mm.

In our experiments the frequency n changes from $5s^{-1}$ to $1000s^{-1}$. The phases of deformation of the capsule are shown in Fig. 18. The direction of the worm motion is opposite to the direction of the travelling magnetic field.

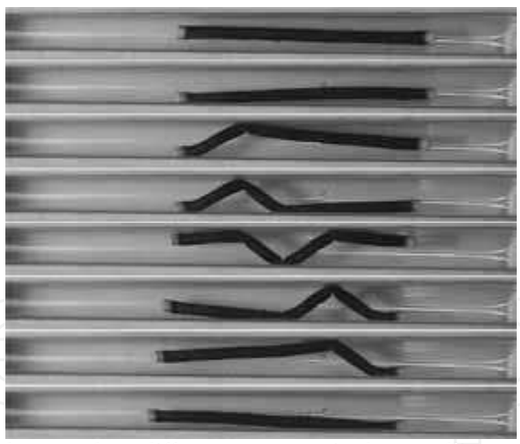

Fig. 18. The form of the capsule at different moments in the travelling magnetic field

The body velocity depends on the geometrical shape of the deformed body and that of the channel. If n is small enough and the body inertia does not affect the body velocity, the following formula is valid:

$$v = k_s(l_s - L)/t_c\ , \quad t_c = (k_s + 3)T\ , \quad k_s = [l_w/l_s]\ . \tag{32}$$

Here l_s is the segment length (a segment is a part of deformed body between two neighbouring coils), k_s is number of the segments, The symbol $[\cdots]$ denotes the integral part of the number, t_c is the time of a cycle. The length of the segment may be determined under assumption about it's form. A segment form is determined by the elastic and magnetic properties of the body material, and the value of the magnetic field.
The problem of determination of the body form is very complex and here we consider three assumptions about the segment form.

Sinusoidal Form

Let us assume that the segment of the body between two coils has sinusoidal form. In this case the equation of the central line of the segment is as follows:

$$y_S = 0.5(d - d_w)\sin(\pi x/L)\ . \tag{33}$$

For parameters $L = 10\text{mm}$, $d = 11\text{mm}$, $l_w = 48\text{mm}$, $d_w = 4\text{mm}$ the length of the sinusoidal segment is $l_s = 12.6\text{mm}$, $k_s = 4$. The analytical estimation of the body velocity is determined as $v = 1.46 \cdot n\ \text{mms}^{-1}$.

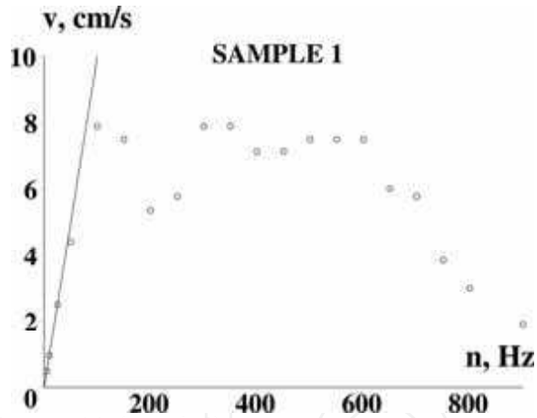

Fig. 19. Body velocity $v = v(n)$ (sample 1)

Body Form is Determined by the Model of Elastic Beam

Let us assume that the form of the segment of the body between two coils is determined by the model of the elastic beam without extension (the bending moment is due to the magnetic forces, assuming that magnetic forces act on the ends of the segment). In this case the equation of the central line of the segment is as follows:

$$y_E = ax^3 + bx^2 + d_w/2\ , \tag{34}$$

where $a = -2(d - d_w)/L^3$, $b = 3(d - d_w)/L^2$. For this assumption and for parameters as above the length of the segment is equal to 12.5mm , $k_s = 4$ and the analytical estimation of the body velocity is $v = 1.43 \cdot n$ mms^{-1}.

Body Form is a Broken Line

Let us assume that the form of the body segment between two coils is a straight line. The equation of the central line of the segment is as follows:

$$y_R = (d - d_w)x/L \,. \tag{35}$$

In this case for parameters as above the length of the segment is 12.2mm , $k_s = 4$ and the analytical estimation of the body velocity is $v = 1.26 \cdot n$ mms^{-1}. From Fig. 19 we can see that for $n < 100s^{-1}$ the theoretical result (the body form is determined by the model of an elastic beam) matches with the experimental data for the sample 1 for the first experiment. The maximal obtained body velocity is $v = 7.89$ cms^{-1} for $n = 100s^{-1}$. For $n > 950s^{-1}$ in the first experiment sample 1 does not move.

From the second experiment it follows that the segment form of the capsule is a straight line. The length of the segment is determined by the formula

$$l_s = \sqrt{L^2 + (d - d_c)^2} = 11.66\text{mm} , \quad k_s = 6 \,. \tag{36}$$

From (20) we find dependency of the velocity of the body on n $v = 1.1 \cdot n$ mms^{-1}. The theoretical dependency of the velocity of the body v on n and experimental data are shown in Fig. 20.

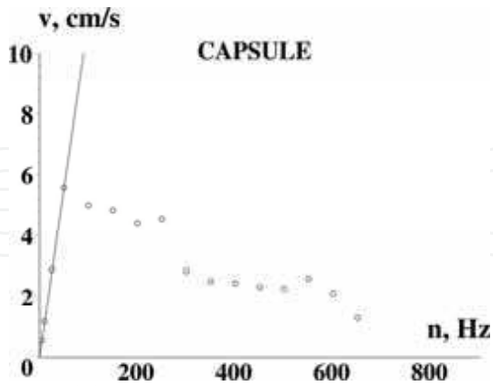

Fig. 20. Body velocity $v = v(n)$ (a capsule with a magnetic fluid)

For the frequency $n < 50s^{-1}$ the theoretical estimation of the velocity of the capsule matches with the experiments. In our experiment for $n > 700s^{-1}$ the capsule does not move. The maximal obtained capsule velocity is $v = 5.56\,\mathrm{cms}^{-1}$ for $n = 50s^{-1}$. The body velocity depends on the geometrical shape of the deformed body and that of the channel. Only if n is small enough the body inertia does not affect the body velocity and the formula (32) is valid. A simulation of the dynamic behavior of the elastic body was made by Finite-Element-Method (Fig. 21). For $n < 100\mathrm{Hz}$ the numerical results coincide with experimental data.

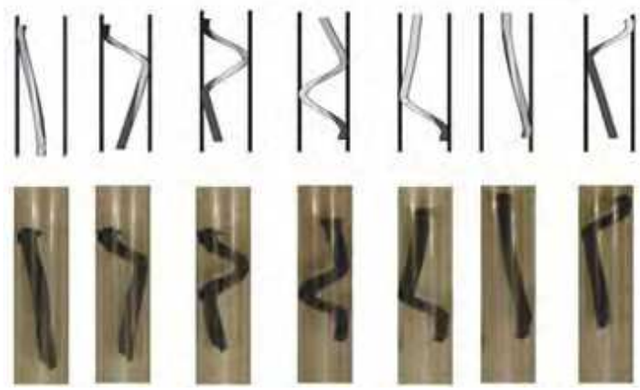

Fig. 21. Analysis of the locomotion (sample 1) for $n < 100\mathrm{Hz}$ using Finite-Element- Method

The Finite-Element-Method is also a useful tool to define optimal control frequencies for the cascaded system of the coils (switching frequencies). As it is shown in Fig. 22 there exists a correlation between the measured velocity of the worm, the switching frequencies of the coils and the eigenfrequencies of the worm respectively.

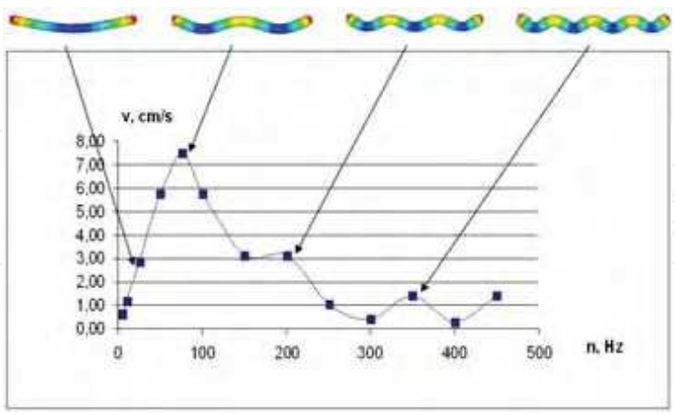

Fig. 22.The velocity of the worm vs. eigenfrequencies (switching frequencies of the coils)

Finally, we should remark that the type of locomotion realized with the magnetic elastomer or the elastic capsule filled with ferrofluid is a snake-like motion called *concertina motion*.

3.5 Design of Active and Passive Locomotion Systems and the Interaction between a Controlled Magnetic Field and a Magnetic Fluid

A moving magnetic field can generate a travelling wave on the surface of magnetic fluids. This travelling wave can be useful as a drive for locomotion systems. Therefore, peristaltically moving active locomotion systems could be realized with an integrated electromagnetic drive (see Fig. 23, left (A)). Also passive locomotion systems can be taken into account. Objects, which are on the surface of the fluid or are lying in the fluid, could be carried floating and/or shifting (see Fig. 23, left (B) and Fig. 26, 27).

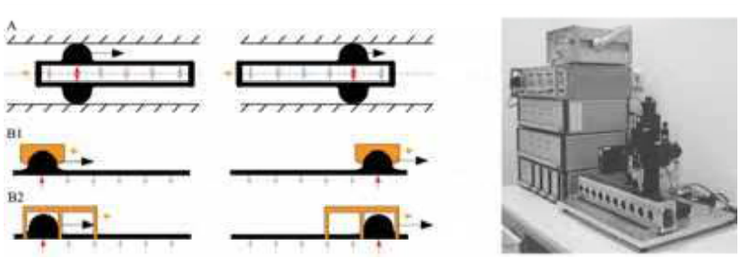

Fig. 23. Schema of possible locomotion systems (left), and the experimental setup (right)

The following properties are important for the locomotion: (i) mass and geometry of the moving or moved object, (ii) the change of the shape and the position of the magnetic fluid, and (iii) the pressure distribution of the magnetic fluid with respect to the action of the moving magnetic field.

To analyse the behavior of the magnetic fluids (under the described action of the magnetic field) and such locomotion systems, the experimental setup consists of 20 consecutively arranged cascaded electromagnets (1 coil generates 3000 ampere turns).

The measurement system to detect the pressure of the fluid and the optical system to analyse the shape of the fluid are connected to a 3 axis-positioning unit (see Fig. 23, right). Fig. 24 shows a travelling wave in a magnetic field.

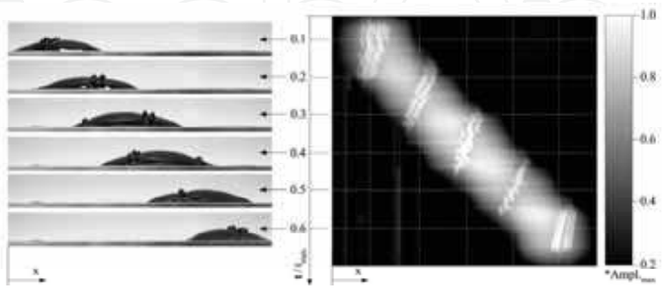

Fig. 24. Travelling wave generated by a moving magnetic field

Fig. 25 shows schematically the magnetic field, which emerges from an electromagnet, the shape of the fluid and the pressure distribution.

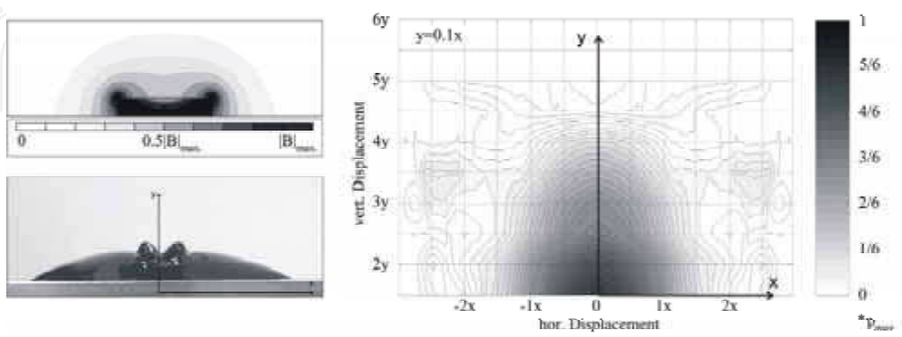

Fig. 25. Schematical presentation of the electric induction density of an excited coil (left top), the emerged shape of the magnetic fluid surface (left bottom), and the pressure distribution of the magnetic fluid (right)

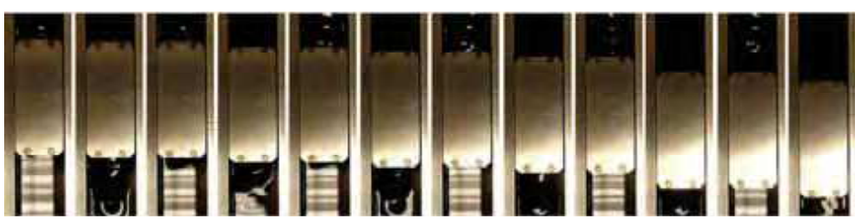

Fig. 26. Example of a passive locomotion by means of travelling waves in a magnetic fluid

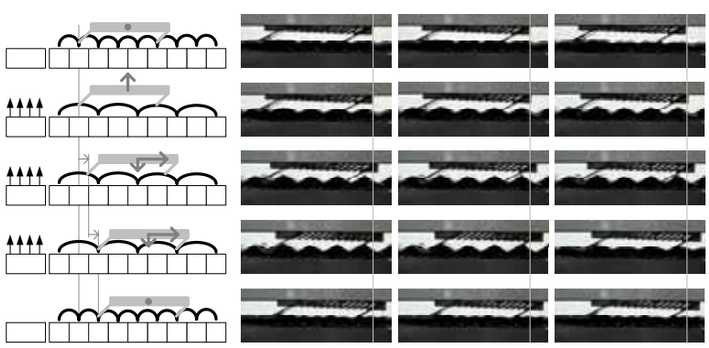

Fig. 27. Functional principal of a passive locomotion system (form of the magnetic field (l.) and the corresponding video sequences (r.))

In the experimental setup using a water–based ferrofluid a maximal change of the fluid pressure about 2200 MPa was measured in the origin (see Fig. 25, right) after applying the magnetic field. Thus, it could be a realistic scenario to construct a cascaded structure of cylindrical membranes filled with a magnetic fluid ("worm") and to get the necessary interaction between "worm" and the environment for peristaltic locomotion.

3.6 Conclusional Remarks

The expression for the magnetic field strength creating a sinusoidal wave on the surface of a viscous magnetic fluid as a function of the characteristics of the fluid (viscosity, surface tension, and magnetic permeability) and the parameters of the wave are obtained.
It is experimentally shown that in a specially structured periodic travelling magnetic field a cylindrical magnetizable elastic body moves along the channel. The direction of the body motion is opposite to the direction of the travelling magnetic field.

The maximal obtained body velocity is $v = 10\,\mathrm{cms}^{-1}$ for $n = 250 s^{-1}$. For the frequency $n < 100 s^{-1}$ (samples 1) and for $n < 50 s^{-1}$ (the capsule with the magnetic fluid) the theoretical (analytical and numerical) estimations of the velocity of the elastic body (the capsule with the magnetic fluid) coincide with the experimental data.
The creation of active biologically inspired locomotion systems and new principle for a passive motion is possible using the deformation deformable magnetizable media in controlled magnetic fields.

4. Summary and Outlook

At the beginning of the chapter it was mentioned that the motion of an earthworm was the inspiration for a technical solution of an artificial worm. A theory is developed for the peristaltic motion of such systems, which to a large extent allows to characterize these motions already on a kinematic level. The advantage of adaptive control for the dynamical realization of these motions is shown. Experiments using a simple prototype checked the results of the theory.
Using magnetizable materials in compliant structures rather snake-like motion (concertina movement) has been realized until now. Since the peristaltic crawling of the earthworm has many advantages for the locomotion in difficult environments the realization of such a motion remains a challenge in theory and control as well as in experiments (Fig. 28).

Fig. 28. From the snake-like concertina motion to worm-like peristaltic crawling

This also applies to the technological realization of an enveloping membrane structure for the artificial worm.

Here two problems (and actually opposite demands) are to be solved:

- membrane thickness as small as possible, to achieve a big force extraction and a very flexible worm structure and
- membrane thickness as big as possible, to avoid diffusion processes of the ferrofluid through the membrane and to keep environmental influences away from the ferrofluid to improve the long-term stability of the worm system.

The objective is to find optimal parameters and to verify these experimentally.
Another challenge for future research is to realize two-dimensional (planar) motions using ferrofluids.

5. References

Abaza, K. (2006). Ein Beitrag zur Anwendung der Theorie undulatorischer Lokomotion auf mobile Roboter – Evaluierung theoretischer Ergebnisse an Prototypen, *PhD thesis*, Faculty of Mechanical Engineering, TU Ilmenau

Behn, C. (2005). *Ein Beitrag zur adaptiven Regelung technischer Systeme nach biologischem Vorbild*, Cuvillier, Göttingen

Behn, C. & Zimmermann, K. (2006). Adaptive lambda-tracking for locomotion systems, *Robotics and Autonomous Systems*, 54, pp. 529-545

Blekhman, I.I. (2000). *Vibrational Mechanics: Nonlinear Dynamic Effects, General Approach, Applications*, World-Scientific, Singapore

Choi, H.R.; Ryew, S.M.; Jung, K.M., Kim, H.M.; Jeon, J.W., Nam, J.D.; Maeda, R. & Tanie, K. (2002). Microrobot actuated by soft actuators based on dielectric elastomer, *Proceedings of IEEE/RSJ International Conference on Intelligence Robots and System*, 2, pp. 1730-1735

Dragan, V. & Halanay, A. (1999). *Stabilization of Linear Systems*, Birkhäuser, Boston

Kato, T.; Nakamura, T.; Iwanaga, T. & Muranaka, Y. (2006). Peristaltic Crawling Robot Based on the Locomotion Mechanism of Earthworms. *Proc. of the 4th IFAC Symposium on Mechatronics*, Heidelberg, September 12-14, 2006, pp. 139-144

Mangan, E.V.; Kingsley, D.A.; Quinn, R.D. & Chiel, H.J. (2002). Development of a peristaltic endoscopies, *Proceedings of IEEE International Conference on Robotics and Automation*, 1, pp. 347-352

Menciassi, A. & Dario, P. (2003). Bio-inspired solutions for locomotion in the gastro-intestinal tract: background and perspectives, *Phil. Trans. R. Soc. London*, A 361, pp. 2287-2298

Miller, G. (1988). The motion dynamics of snakes and worms, *Computer Graphics*, 22, pp. 169-173

Miller, D.E. & Davison, E.J. (1991). An adaptive controller which provides an arbitrary good transient and steady-state response, *IEEE Transaction on Automatic Control*, 36, pp. 68-81

Ostrowski, J.P.; Burdick, J.W., Lewis, A.D. & Murray, R.M. (1995). The mechanics of undulatory locomotion: the mixed kinematic and dynamic case, *Proceedings of IEEE International Conference on Robotics and Automation*, pp. 1945-1951, Nagoya, May, 1995, Japan

Naletova, V.A., Kvitantsev, A.S. & Turkov, V.A. (2003). Movement of a magnet and a para-magnetic body inside a vessel with a magnetic fluid. *J. Magn. Magn. Mater.,* 258-259, pp. 439-442

Naletova, V.A., Turkov, V.A. & Tyatyushkin, A.N. (2005). Spherical body in a magnetic fluid in uniform electric and magnetic fields. *J. Magn. Magn. Mater.,* 289, pp. 370-372

Naletova, V.A., Kvitantsev, A.S. (2005). Thermomagnetic force acting on a spheroidal body in a magnetic fluid. *J. Magn. Magn. Mater.,* 289, pp. 250-252

Popp, J. (2006). Ferrofluide und Ferrogele – Neue Materialien in der Anwendung für Lokomotions- und Manipulationssysteme. *Diploma Thesis*, Faculty of Mechanical Engineering, TU Ilmenau

Rosensweig, R.E. (1985). *Ferrohydrodynamics*, Cambridge University Press, Cambridge

Raj K. , Moskowitz B. (1990). Commercial applications of ferrofluids, *J. Magn. Magn. Mater.,* 85, pp. 233–245.

Raj K. , Moskowitz B. , Casciari R.(1995). Advances in ferrofluid technology, *J. Magn. Magn. Mater.,* 149 (1–2), pp.174–180.

Saga, N. & Nakamura, T. (2002). Elucidation of propulsive force of micro-robot using magnetic fluid, *J. Appl. Phys.*, 91, pp. 7003-7005

Saga, N. & Nakamura, T. (2004). Development of a peristaltic crawling robot using magnetic fluid on the basis of locomotion mechanism of the earthworm, *Smart Mater. Struct.*, 13, pp. 566-569

Steigenberger, J. (1999). On a class of biomorphic motion systems, *Preprint No. M12/99*, Faculty of Mathematics and Natural Sciences, TU Ilmenau, Germany

Steigenberger, J. (2004). Modelling artificial worms, *Preprint No. M02/04*, Faculty of Mathematics and Natural Sciences, TU Ilmenau, Germany

Steigenberger, J. (2003). Contribution to the mechanics of worm-like motion systems and artificial muscles, *Biomech. and Modeling in Mechanobiology*, 2, pp. 37-57

Turkov, V.A. (2002). Deformation of an elastic composite involving a magnetic fluid, *J. Magn. Magn. Mater.*, 252, pp. 156-158

Weiting, L.; Menciassi, A.; Scapellato, S.; Dario, P.; Yuquan Chen (2006). A biomimetic sensor for crawling. *Robotics and Autonomous Systems*. 54, pp. 513-528

Ye, X. (1999). Universal lambda-tracking for nonlinearly-perturbed systems without restrictions pn the relative degree, *Automatica*, 35, pp. 109-119

Zimmermann, K.; Steigenberger, J. & Zeidis, I. (2002). Mathematical model of worm-like motion systems with finite and infinite degree of freedom, *Proceedings of 14th CISM-IFToMM Symposium on Theory and Practice of Robots and Manipulators (RO-MANSY)*, pp. 507-515, Udine, July, 2002, Italy

Zimmermann, K.; Steigenberger, J. & Zeidis, I. (2003). On artificial worms as a chain of mass points, *Proceedings of 6th International Conference on Climbing and Walking Robots (CLAWAR)*, pp. 11-18, Catania, September, 2003, Italy

Zimmermann, K.; Zeidis, I., Naletova, V.A. & Turkov, V.A. (2004). Waves on the surface of a magnetic fluid layer in a travelling magnetic field, *J. Magn. Magn. Mater.*, 268, pp. 227-231

Zimmermann, K.; Zeidis, I.; Naletova, V.A. & Turkov, V.A. (2004). Travelling waves on a free surface of a magnetic fluid layer, *J. Magn. Magn. Mater.*, 272-276, pp. 2343-2344

Zimmermann, K.; Zeidis, I.; Naletova, V.A. & Turkov, V.A. (2004). Modelling of worm-like motion systems with magneto-elastic elements, *Phys. Stat. Solid.*, 1, pp. 3706-3709

Zimmermann K.; Naletova V.A., Zeidis I.; Böhm, V.; Kolev, E. (2006). Modelling of locomotion systems using deformable magnetizable media. *J. of Physics: Cond. Matter*, 18, pp. 2973–2983

Zimmermann, K.; Zeidis, I.; Naletova, V.A.; Turkov, V.A.; Bachurin, V.E. (2004). Locomotion Based on a Two-layers Flow of Magnetizable Nanosuspensions. *Proceedings of the JEMS'04, Joint European Magnetic Symposia*, September, 5-10, Dresden, Germany, pp. 134

Zimmermann, K.; Naletova, V.A.; Zeidis, I.; Turkov, V.A.; Kolev, E.; Lukashevich, M.V.; Stepanov, G.V. (2007). A deformable magnetizable worm in a magnetic field – a prototype of a mobile crawling robot. *J. Magn. Magn. Mater.* 311, pp. 450-453

Climbing and Walking Robots: towards New Applications

Edited by Houxiang Zhang

ISBN 978-3-902613-16-5

Hard cover, 546 pages

Publisher I-Tech Education and Publishing

Published online 01, October, 2007

Published in print edition October, 2007

With the advancement of technology, new exciting approaches enable us to render mobile robotic systems more versatile, robust and cost-efficient. Some researchers combine climbing and walking techniques with a modular approach, a reconfigurable approach, or a swarm approach to realize novel prototypes as flexible mobile robotic platforms featuring all necessary locomotion capabilities. The purpose of this book is to provide an overview of the latest wide-range achievements in climbing and walking robotic technology to researchers, scientists, and engineers throughout the world. Different aspects including control simulation, locomotion realization, methodology, and system integration are presented from the scientific and from the technical point of view. This book consists of two main parts, one dealing with walking robots, the second with climbing robots. The content is also grouped by theoretical research and applicative realization. Every chapter offers a considerable amount of interesting and useful information.

How to reference

In order to correctly reference this scholarly work, feel free to copy and paste the following:

Klaus Zimmermann, Igor Zeidis, Joachim Steigenberger, Carsten Behn, Valter Boehm, Jana Popp, Emil Kolev and Vera A. Naletova (2007). Worm-like Locomotion Systems (WLLS) - Theory, Control and Prototypes, Climbing and Walking Robots: towards New Applications, Houxiang Zhang (Ed.), ISBN: 978-3-902613-16-5, InTech, Available from: http://www.intechopen.com/books/climbing_and_walking_robots_towards_new_applications/worm-like_locomotion_systems__wlls__-_theory__control_and_prototypes

INTECH
open science | open minds

InTech Europe
University Campus STeP Ri
Slavka Krautzeka 83/A
51000 Rijeka, Croatia
Phone: +385 (51) 770 447
Fax: +385 (51) 686 166
www.intechopen.com

InTech China
Unit 405, Office Block, Hotel Equatorial Shanghai
No.65, Yan An Road (West), Shanghai, 200040, China
中国上海市延安西路65号上海国际贵都大饭店办公楼405单元
Phone: +86-21-62489820
Fax: +86-21-62489821

IntechOpen